AIAA JOURNAL
Vol. 39, No. 4, April 2001

Effects of Passive Porous Walls on Boundary-Layer Instability

Peter W. Carpenter*
University of Warwick, Coventry, England CV4 7AL, United Kingdom
and
Lee J. Porter†
British Aerospace plc., Bristol, England BS12 7QW, United Kingdom

A theoretical study is described of the effects of a passive porous wall on boundary-layer instability. The passive porous wall is conceived of as a thin porous sheet stretched over a plenum chamber. When disturbances in the form of Tollmien–Schlichting waves propagate along the boundary layer, the fluctuating pressure forces air in and out of the plenum chamber. The basic approach is based on classic linear stability theory for the flat-plate boundary layer with modified wall boundary conditions. The wall response is represented by a complex admittance (ratio of fluctuating flow rate per unit area to wall pressure) and, therefore, applies to a general class of passive porous, and other interactive, walls. The effects of a wide range of admittance values are studied. A stabilizing effect is obtained when the admittance phase is close to $\pi/2$, and an optimum value of admittance magnitude is also found. A theoretical model is introduced and used to calculate the admittance of the porous panels used in a parallel experimental study. It is shown that it may be possible to manufacture stabilizing porous panels. The stabilizing mechanism is due to the production of a near-wall region of negative Reynolds stress.

Nomenclature

D, D^2, D^3	=	$\mathrm{d}/\mathrm{d}y, \mathrm{d}^2/\mathrm{d}y^2, \mathrm{d}^3/\mathrm{d}y^3$
$\mathcal{E}$	=	$\exp\{i(\alpha x - \omega t)\}$
F	=	$(\omega/Re) \times 10^6$
h	=	depth of plenum chamber
$\bar{h}$	=	h/δ^*
i	=	$\sqrt{(-1)}$
p	=	dimensionless pressure fluctuation
q_w	=	dimensionless flow rate per unit area through wall
Re	=	$U_\infty \delta^*/\nu$
t	=	dimensionless time
U	=	undisturbed streamwise velocity component
U_∞	=	freestream flow speed
u	=	dimensionless fluctuating streamwise velocity component
v	=	dimensionless fluctuating normal velocity component
x	=	dimensionless streamwise coordinate
Y_b	=	$\hat{q}_w/\hat{p}_w$
Y_c	=	$\hat{q}_w/\hat{p}_c$
Y_p	=	$\hat{q}_w/(\hat{p}_w - \hat{p}_c)$
Y_w	=	wall admittance; see Eq. (1)
$\bar{Y}_w$	=	wall admittance magnitude
y	=	dimensionless coordinate normal to wall
α	=	dimensionless disturbance wave number
β	=	$\sqrt{(\alpha^2 - i\omega/\nu)}$
δ^*	=	boundary-layer displacement thickness
ζ	=	dimensionless disturbance vorticity
η	=	dimensionless compliant wall displacement
μ	=	dynamic viscosity
ν	=	kinematic viscosity
ρ	=	density
σ	=	wall porosity, that is, proportion of area occupied by pores
φ	=	admittance phase
ω	=	dimensionless disturbance frequency

Subscripts

c	=	quantities evaluated in the plenum chamber
i	=	imaginary part
r	=	real part
w	=	quantities evaluated at the wall
$\sigma = 1$	=	quantities evaluated with $\sigma = 1$

Superscripts

$\hat{}$	=	disturbance amplitude
$\bar{}$	=	average over a disturbance cycle

I. Introduction

THE classic model for laminar–turbulent transition was formulated by Prandtl, Tollmien and Schlichting, and confirmed by the experiments of Schubauer and Skramstadt (see Ref. 1). According to this model, the natural transition process begins with quasi-random pointlike disturbances that generate packets of low-amplitude, quasi-two-dimensional, Tollmien–Schlichting waves through some unspecified receptivity mechanism. Many other routes to transition are now known. Nevertheless, the classic model remains valid for boundary layers that are not too far removed from the two-dimensional flat-plate case and that develop in a low-noise environment. Such conditions are to be found, for example, on aircraft in free flight.

Why do the Tollmien-Schlichting waves grow? Essentially, it is because energy is transferred irreversibly to the disturbances. The mechanism is the so-called energy production by the Reynolds stresses. If the rate of energy production exceeds the rate of energy removal due to viscous dissipation, the waves will grow. However, in the absence of viscosity, the streamwise and normal velocity perturbations, u and v, respectively, are out of phase by exactly 90 deg. Under these conditions, the Reynolds stress would be zero, and no energy would be transferred to the disturbance. The necessary phase change for disturbance growth is brought about by viscous effects in the critical layer. This prompts one to speculate on whether it would be possible to postpone or eliminate transition by interfering in some way with this phase change, to reverse it, partly or fully, thereby reducing or even changing the sign of the Reynolds stress. In fact, it is already known that this is the main reason that wall compliance can stabilize Tollmien–Schlichting waves[2,3] and other instabilities.[4,5]

One possible way to interfere with the phase relationship between u and v is by means of a passive porous wall of the type

Received 3 November 1999; revision received 18 July 2000; accepted for publication 2 August 2000. Copyright © 2000 by the American Institute of Aeronautics and Astronautics, Inc. All rights reserved.

*Professor of Mechanical Engineering, School of Engineering. Senior Member AIAA.

†Research Aerodynamicist, Sowerby Research Centre, Mathematical Modeling Department.

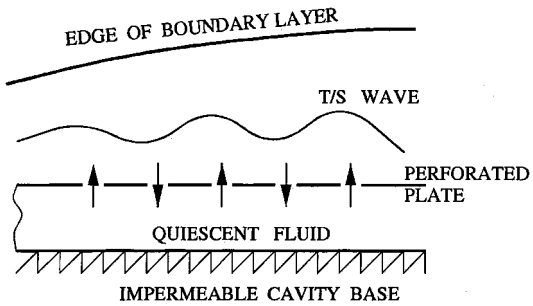

Fig. 1 Schematic of the passive-porous-wall mechanism.

shown in Fig. 1. This consists of a very thin perforated plate or sheet stretched over a plenum chamber. As they propagate along the boundary layer, Tollmien–Schlichting waves create a fluctuating pressure field, which drives small quantities of air through the perforated sheet in and out of the plenum chamber. A fundamental quantity for characterizing the response of the passive porous wall to the Tollmien–Schlichting waves is the admittance, defined as follows:

$$Y_w = \frac{\text{fluctuating flow rate per unit area through wall}}{\text{fluctuating pressure acting on the wall}} \tag{1}$$

The key questions addressed in the present paper are whether there are complex values of admittance such that Tollmien–Schlichting waves are stabilized, and whether it is possible to manufacture passive porous walls that stabilize Tollmien–Schlichting waves.

The concept of using the sort of passive porous wall shown schematically in Fig. 1 for transition postponement appears to be novel. However, certain aspects of the theoretical modeling are quite similar to the approach devised by Gaponov[6–8] and Lekoudis[9] to model the effect of a permeable surface on boundary-layer stability. In the theoretical work on the effect of suction on boundary-layer stability previous to theirs, it was usually assumed that the fluctuating velocity at the wall was zero. Gaponov[6–8] and Lekoudis[9] recognized that this could be a poor assumption in some cases, especially when the suction slots connected the boundary layer to a plenum chamber. They pointed out that as Tollmien–Schlichting waves traveled along the boundary layer they would have driven a fluctuating component of flow through the slots. This fluctuating flow would be superimposed on the steady suction flow. The correct boundary condition at the wall should have taken this fluctuating component into account. This then led to a formulation of the boundary-layer stability problem, which in certain respects is similar to that developed in the present paper. In the more recent work of Carpenter,[10] which in a sense is preliminary to the present paper, the flow in the pores of the passive porous walls was modeled using unsteady pipe-flow theory or its two-dimensional equivalent. It was found that the greatest stabilizing effect is obtained with inclined pores. However, it was also found that the necessary admittance values could only be realized in practice by using very short pores, which violates the assumptions behind unsteady pipe-flow theory and also makes the use of inclined pores impractical. In the present paper we assume that the porous surface is made from thin sheet, thereby ensuring the pores are very short.

There has also been a certain amount of work on other applications of passive porous walls for drag reduction. For instance, Schetz and Kong,[11] Wilkinson,[12] and Collier and Schetz[13] carried out experimental investigations on the use of such walls to reduce drag for fully turbulent boundary layers. The porous walls took the form of perforated plates over adjustable plenum chambers. Drag increase was observed in all cases tested. The use of passive porous walls for drag control in transonic flow has also been studied experimentally by Nagamatsu et al.[14] and Breitling and Zierep.[15] Similarly, ventilated porous walls have long been used to reduce blockage effects in transonic tunnels (for example, see the recent paper by Beutner et al.[16]). In this case the passive porous walls were effective at reducing shock strength and, thereby, wave drag. Finally, a number of passive porous-wall drag-reduction mechanisms were proposed by Bechert et al.[17] in their study of the hydrodynamics of shark skin.

The remainder of the paper is organized in the following way. In Sec. II, we present a general inverse theory to study the effects of varying admittance magnitude and phase on Tollmien–Schlichting waves. In Sec. III, a theoretical model is presented for determining the admittance for the type of passive porous surface being used in a parallel experimental study. This model is used to study the effects of such walls on the evolution of Tollmien–Schlichting waves and to provide a physical explanation for their stabilizing properties. Finally, conclusions are given in Sec. IV.

II. General Inverse Theory

A. Formulation

The stability of a boundary layer on a flat plate with a passive porous wall is considered. The usual assumption of quasi-parallel flow is made. It is assumed that in the absence of a disturbance the pressure difference across the passive porous wall would equilibriate, making the mean flow identical to that for an impermeable wall, so that the Blasius solution is the undisturbed velocity profile. It is further assumed that the disturbance is sufficiently small for the governing equations to be linearized and that it takes the form of a two-dimensional traveling wave, so that the velocity and pressure fluctuations can be written in the form:

$$\{u, v, p\} = \{\hat{u}, \hat{v}, \hat{p}\}\mathcal{E} + \text{c.c.} \qquad \text{where} \qquad \mathcal{E} = \exp\{i(\alpha x - \omega t)\} \tag{2}$$

where $\alpha = (\alpha_r + i\alpha_i)$ is the complex wave number, with α_r the physical wave number and $-\alpha_i$ the growth rate of the disturbance with respect to the streamwise direction x, and c.c. is the complex conjugate. All quantities are made nondimensional using the freestream speed U_∞, density ρ, kinematic or dynamic viscosity, ν or μ, and boundary-layer displacement thickness δ^*.

The assumptions made are standard for classic linear hydrodynamic stability theory. Therefore, it follows that $\hat{v}$ is governed by the well-known Orr–Sommerfeld equation. The usual boundary conditions, requiring exponential decay of the disturbance velocity, are assumed at the outer edge of the boundary layer. At the wall, kinematic boundary conditions are imposed requiring continuity in the disturbance velocity between the boundary layer and q_w, the flow rate per unit area entering the porous wall. Thus,

$$\hat{u}_w = 0 \tag{3a}$$

$$\hat{v}_w = -\hat{q}_w \tag{3b}$$

These boundary conditions are similar to those derived for the compliant wall,[3,18,19] provided that the substitution $\hat{q}_w = i\omega\hat{\eta}$ is made, where $\hat{q}_w$ and $\hat{\eta}$ are the amplitudes of q_w and of the dimensionless vertical wall displacement. There is, however, one crucial difference; for a compliant wall, $\hat{u}_w$ in Eq. (3a) is replaced by $\hat{u}_w + DU_w\hat{\eta}$ where DU_w is the undisturbed velocity gradient at the undisturbed wall position. The additional term reflects that in the case of the compliant wall the surface moves under the action of the fluctuating forces. The difference between the form of the boundary condition (3a) for the two cases appears to be almost trivial, but, in fact, has important consequences.

The formulation of the problem is completed by introducing the concept of admittance [see Eq. (1)]. The wall admittance is a complex number that characterizes the way the porous wall (or compliant wall) responds to a fluctuating pressure acting on the upper surface. Thus, the admittance evaluated from the boundary-layer side can be written as

$$Y_b = \hat{q}_w/\hat{p}_w \tag{4}$$

The form used in Eq. (4) is equivalent that used in studies of the effects of wall compliance on boundary-layer stability and transition.[3,18]

At the wall the admittance evaluated from the boundary-layer side must equal the admittance of the porous wall, so that, using Eqs. (3b) and (4), the additional boundary condition at the wall becomes

$$Y_b = Y_w \qquad \text{or} \qquad Y_w\hat{p}_w + \hat{v}_w = 0 \tag{5}$$

where $\hat{p}_w$ can be written in terms of $\hat{v}_w$ (Ref. 3); thus,

$$\hat{p}_w = 1/(\alpha^2 Re)\left[D^3\hat{v}_w - \alpha^2 D\hat{v}_w + iRe(\alpha\hat{v}_w DU_w + \omega D\hat{v}_w)\right] \quad (6)$$

where $Re = \delta^* U_\infty/\nu$ and D, D^2, and D^3 are the first, second, and third derivatives with respect to y.

Thus $\hat{v}_w$ and $\hat{p}_w$ can be evaluated from the solution to the Orr–Sommerfeld equation. This equation with its two outer boundary conditions and the wall conditions (3a) (3b), and (5) form an eigenproblem for which α is the complex eigenvalue and $\hat{v}$ is the complex eigenfunction. Equation (5) could be regarded as the eigenvalue equation and takes the form

$$F(\alpha; \omega, Re, Y_w) = 0 \quad (7)$$

The aim is to calculate the complex values of α for specified values of ω and Re and a range of complex values of admittance with the view, in particular, of determining how the disturbance growth rate $-\alpha_i$ varies.

B. Numerical Methods

The eigenvalue equation (7) has to be solved numerically. Two completely independent methods were used. This had great advantage for validation of the results. Complete agreement was found using the two methods. The first method, used by Carpenter,[10] is based on the scheme developed by Carpenter and Morris,[3] which combines a shooting method with orthonormalization for the numerical integration of the Orr–Sommerfeld equation. This is coupled with the method of false position to solve Eq. (7) iteratively. The second method, also used by Carpenter and Morris, is based on a Chebyshev spectral scheme and is closely modeled on that of Bridges and Morris.[20] This can be used to achieve a globally convergent scheme, which was used to check if there were any additional unstable eigensolutions. Mostly, however, Bridges and Morris's[20] local iteration scheme[3] was used to solve Eq. (7). The required modifications to accommodate the slightly different boundary conditions for the passive porous wall are very straightforward.

In common with the work on the effects of wall compliance on boundary-layer instabilities, for example, Carpenter and Morris,[3] we found that considerably smaller step sizes were required to achieve a given accuracy for passive porous walls as compared with impermeable rigid walls. In all cases a careful study was undertaken to ensure that a sufficient number of steps were taken to achieve the required accuracy, and good agreement was found with the previously published results for the impermeable rigid wall. Also good agreement was found between the shooting and spectral methods for the passive porous walls. Typically, for the shooting method it was found that 500 steps were required for a passive porous wall to obtain the same accuracy as achieved with 200 steps for the impermeable rigid wall. Similarly for the spectral code, 65 Chebyshev polynomials were needed to achieve a relative accuracy of less than 0.01, whereas only 35 were needed for the rigid impermeable wall. We experienced difficulties obtaining converged solutions using the spectral scheme for relatively large porosities when α_i became positive, that is, for damped solutions.

C. Physical Interpretation of the Wall Admittance

The wall admittance is complex and is conveniently written in the form

$$Y_w = \bar{Y}_w e^{i\varphi} \quad (8)$$

In general, the phase φ of the wall admittance is nonzero, reflecting that the flow through the pore is usually out of phase with the driving pressure. A deeper understanding of how to interpret the value of φ may be obtained by drawing an analogy with the simple forced linear oscillator. In this case the admittance can be defined as the ratio of velocity to driving force, and its phase is given by

$$\varphi = \arctan\left[\left(\omega^2 - \omega_0^2\right)\Big/\gamma\omega\right] \quad (9)$$

where ω_0 is the natural frequency and γ is the damping factor. When $\gamma \to 0$, $\varphi = -\pi/2$ for $\omega < \omega_0$; however, when the resonant frequency is reached, the phase angle jumps to $\pi/2$ so that, for $\omega > \omega_0$, $\varphi = \pi/2$. For low damping, the behavior is approximately the same. Thus, a passive porous wall can be said to be operating in superresonant/subresonant mode when φ is in the approximate vicinity of $\pm\pi/2$, respectively.

The work done by the fluctuating pressure p_w in driving fluid in and out of the wall is given by

$$\tfrac{1}{4}(p_w + \text{c.c.})(q_w + \text{c.c.}) = \tfrac{1}{4}(p_w + \text{c.c.})(Y_w p_w + \text{c.c.})$$

One might expect that for a purely passive wall the net energy transfer should always be from the fluid flow to the wall and that, accordingly, the preceding quantity should be positive when averaged over a cycle or wavelength. For this to be so, the real part of the admittance must be greater than or equal to zero, that is,

$$-\pi/2 \le \varphi \le \pi/2$$

This argument is not, in fact, completely sound because it is quite possible for a passive wall to alter the phase between q_w (or wall displacement in the case of a compliant wall) and the effective driving pressure to allow energy to pass from the wall to the flow. For example, this happens in the case of subcritical traveling-wave flutter over a compliant wall.[2,3,21] In the case of a Tollmien–Schlichting (T–S) wave, the most important energy transfer mechanisms are viscous dissipation and energy production by the Reynolds stress, both of which occur across the bulk of the boundary layer (see Carpenter[2] and Carpenter and Morris[3] for a discussion of energy transfer mechanisms for boundary layers over compliant walls). Thus, it is quite possible for a passive porous or compliant wall to bring about a favorable change in these main energy-transfer mechanisms, leading to a reduction in T–S wave growth rate, while at same time a much smaller amount of energy is transferred from the wall to flow. Under these circumstances φ could be slightly less than $-\pi/2$. Nevertheless, the normal expectation is for φ to lie between $-\pi/2$ and $+\pi/2$ in the case of a passive wall. Accordingly, this is the range of values assumed for presenting the results given next.

D. Results of the Numerical Study

In the general inverse theory, the porous wall is characterized by two (real) parameters: $\bar{Y}_w$ and φ. The immediate objective of the present study is to identify the range of values for these parameters for which there is a beneficial effect on the growth of boundary-layer disturbances in the form of T–S waves. This will allow the suitability of passive porous walls for maintaining laminar flow to be assessed. This approach was inspired by that developed by Sen and Arora[21] for studying the effects of wall compliance on boundary-layer stability.

To solve the eigenvalue equation (7) for the complex eigenvalue α, it is necessary to choose values of ω and Reynolds number Re, as well as $\bar{Y}_w$ and φ. In many ways the most appropriate choice for ω is the frequency of the fastest growing T–S wave, which is the precursor to transition. The corresponding frequency parameter, $F = (\omega/Re) \times 10^6$, is approximately 30, and its growth rate reaches a maximum at $Re \simeq 2240$. These approximate values for the critical T–S wave provide an appropriate choice of ω and Reynolds number.

The globally convergent eigenvalue search scheme was used to survey a fairly wide range of frequencies and Reynolds numbers to check whether there are any other unstable eigenmodes for passive porous walls apart from the T–S waves. No other instabilities were found. Figure 2 presents the variation of α_r and α_i with φ for two values of $\bar{Y}_w$ for a passive porous wall. The corresponding results for the compliant and rigid wall are also plotted for comparison. Note that both compliant and porous walls have a beneficial effect, in that the growth rate $-\alpha_i$ falls below the rigid-wall value, when φ is fairly close to $-\pi/2$, that is, in subresonant operating mode with moderate to low damping. For superresonant operation, that is, φ very near $\pi/2$, passive porous walls, but not compliant walls, also have a beneficial effect and, in fact, can completely stabilize the T–S waves. For subresonant operation, compliant walls are considerably more effective than porous walls with the same values of $\bar{Y}_w$ and φ.

The physical reason for the greater effectiveness of compliant walls in the subresonant mode of operation is that the wall actually moves, whereas it does not for the porous wall. This is reflected in the

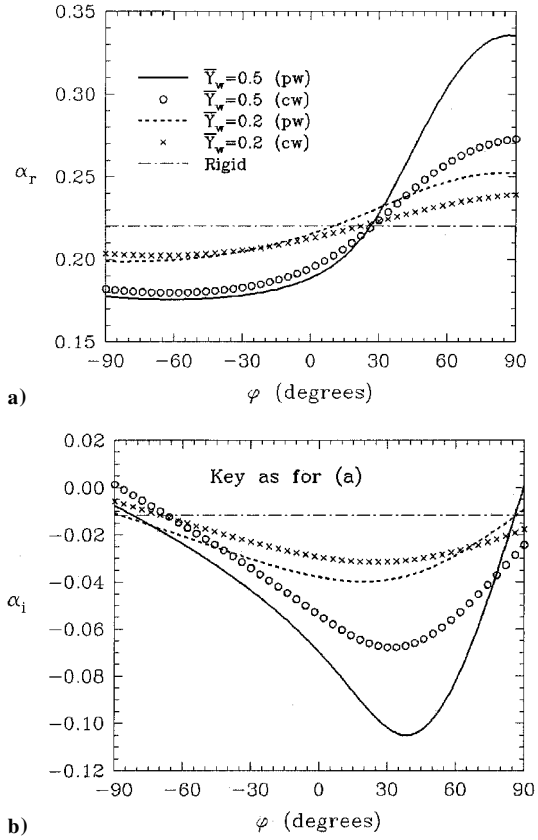

Fig. 2 Variation of α_r and α_i with the phase of the admittance for passive porous walls (PW) and the corresponding compliant walls (CW): $F = 30$ and $Re = 2240$.

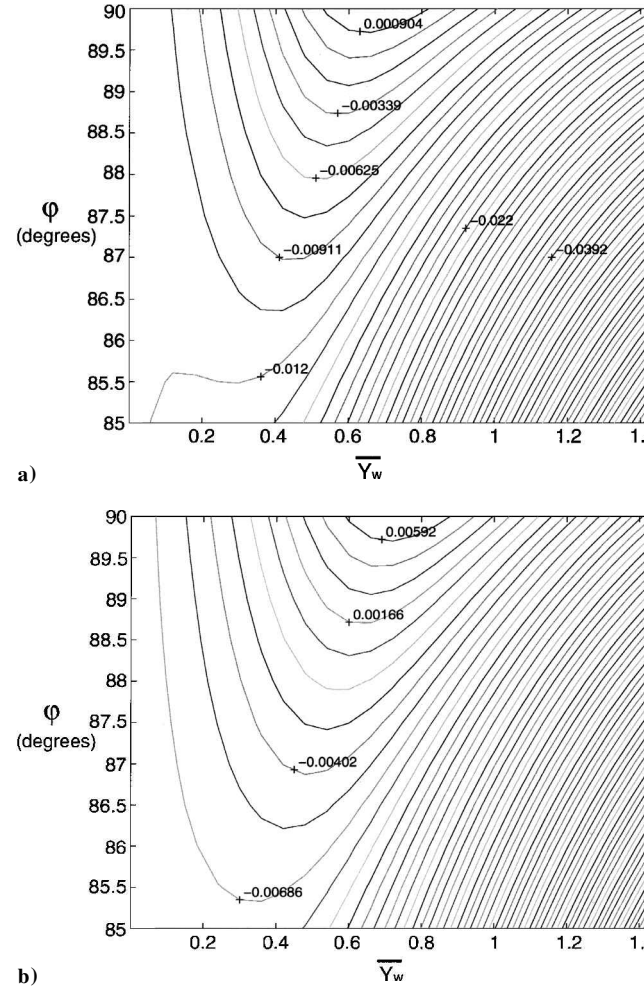

Fig. 3 Contours of $-\alpha_i$ as it varies with admittance magnitude and phase for a superresonant passive porous wall: a) $F = 30$, $Re = 2240$, and rigid-wall value is $-\alpha_i = 0.0117$; and b) $F = 92.2$, $Re = 1060$, and rigid-wall value is $-\alpha_i = 0.0077$.

additional term, discussed earlier, which is required for compliant walls in the no-slip boundary condition (3a). This wall movement leads to substantial additional energy removal which helps to reduce the growth of the T–S wave.[2,3] In fact, the superficial resemblance mathematically between the two types of passive wall, owing to the similarity of the wall boundary conditions, is rather misleading. In practice, it appears that passive porous walls always act superresonantly, whereas compliant walls act subresonantly.[10] Consequently, one may expect the flow physics involved in the two cases to differ markedly.

The variation of α_i with admittance magnitude and phase is plotted in Fig. 3 for a superresonant passive porous wall. Two cases are illustrated. Figure 3a corresponds to the parameters of Fig. 2. The frequency parameter and Reynolds number for Fig. 3b correspond approximately to the conditions of a parallel experimental study. In both cases it can be seen that there is a range of values of the admittance amplitude and phase for which the growth rate of the T–S waves is reduced and a smaller range for which there is complete stabilization, that is, $\alpha_i > 0$. The range of favorable parameters is larger in Fig. 3b than in Fig. 3a. Thus, it has been established that it is possible to stabilize T–S waves with passive porous walls having the appropriate response in terms of admittance. The outstanding question addressed in Sec. III is whether it is possible to achieve such admittance values in practice.

III. Theoretical Model for Passive Porous Walls

A. Expressions for Admittance of Practically Realizable Cases

In the preceding section it has been established that passive porous walls that respond in the appropriate way can substantially reduce the growth of T–S waves. This section addresses the question of whether it is possible to realize such walls in practice. In fact, the theoretical model is developed for the passive porous walls constructed for a parallel experimental study. These walls (see Fig. 1) comprise a very thin porous metal sheet stretched over a plenum chamber. Gaponov[7] has shown that, provided the separation distance between adjacent slots or holes in the porous plate is very much smaller than the wavelength of the T–S waves, the individual slots or holes can be ignored and the flow rate q_w through the wall can be regarded as a continuous function of x. This condition is comfortably met in the porous panels constructed for the study, and it allows us to use the concept of an admittance to formulate the wall-reponse boundary condition.

For the sort of porous wall shown in Fig. 1, there will be two contributions to the wall admittance, namely, that due to the flow through the pores (or holes) in the sheet and that due to the plenum chamber. For the flow through the pores,

$$Y_p \equiv \hat{q}_w/(\hat{p}_w - \hat{p}_c) \tag{10a}$$

For the flow through the plenum chamber,

$$Y_c \equiv \hat{q}_w/\hat{p}_c \tag{10b}$$

where p_w and p_c are the driving pressures at the wall and for the plenum chamber, that is, at the exit of the pores into the chamber, respectively.

The admittance is proportional to the solidity or porosity σ of the porous surface, that is, the fraction of the surface occupied by pores; it is also analogous to the reciprocal of resistance. Thus, Eqs. (10a) and (10b) imply that

$$\hat{p}_w = (\hat{p}_w - \hat{p}_c) + \hat{p}_c = \hat{q}_w\ (1/Y_p) + (1/Y_c)] \tag{11}$$

so that the overall admittance $Y_w (= \hat{q}_w/\hat{p}_w)$ is related to the admittances of the two components as follows:

$$Y_w = \sigma(Y_w)_{\sigma=1} \tag{12a}$$

$$1/(Y_w)_{\sigma=1}] = \ 1/(Y_p)_{\sigma=1}] + \ 1/(Y_c)_{\sigma=1}] \tag{12b}$$

Carpenter[10] used unsteady pipe theory to derive an expression for Y_p. This assumes that the pores are very long compared with their diameter. Here, the opposite extreme is assumed, that is, that the pores are very short compared with their length. Accordingly, $p_w \simeq p_c$, implying $Y_p \gg Y_c$, so that to a good approximation the first term on the right-hand side of Eq. (12b) can be ignored.

B. Expression for Admittance of Plenum Chamber

When the pores connect the boundary layer to a common plenum chamber, a wave-like disturbance also propagates along the chamber. Thus, for an infinitely long plenum chamber, the velocity components of the flow there are written in the form

$$\{u_c, v_c\} = \{\hat{u}_c, \hat{v}_c\}\mathcal{E} + \text{c.c.} = \left\{\frac{i}{\alpha}\frac{\mathrm{d}\hat{v}_c}{\mathrm{d}y}, \hat{v}_c\right\}\mathcal{E} + \text{c.c.} \tag{13}$$

where the continuity equation has been used to write $\hat{u}_c$ in terms of $\hat{v}_c$. In the plenum chamber, the coordinate y is measured downward from the upper surface of the chamber. U_∞, δ^*, etc., are still used to make all quantities nondimensional.

For the flow in the plenum chamber, it can be shown[19] that the linearized Navier–Stokes equations reduce to a single constant-coefficient, fourth-order, ordinary differential equation for $\hat{v}_c$. In fact, this equation is identical to the Orr–Sommerfeld equation with the mean undisturbed velocity set equal to zero. Its general solution takes the following form:

$$\hat{v}_s = A_1 e^{\alpha y} + A_2 e^{-\alpha y} + A_3 e^{\beta y} + A_4 e^{-\beta y} \tag{14}$$

where $\beta = \sqrt{(\alpha^2 - i\omega/\nu)}$ and the A_i, $i = 1, 2, 3, 4$, are constants. The four boundary conditions are

$$\hat{v}_c = -\hat{q}_w \qquad \text{at} \qquad y = 0 \tag{15a}$$

$$\hat{u}_c = 0 \qquad \text{or} \qquad \frac{\mathrm{d}\hat{v}_c}{\mathrm{d}y} = 0 \qquad \text{at} \qquad y = 0 \tag{15b}$$

$$\hat{v}_c = \hat{u}_c = 0 \tag{15c}$$

$$\hat{v}_c = \frac{\mathrm{d}\hat{v}_c}{\mathrm{d}y} = 0 \qquad \text{at} \qquad y = -\bar{h} \tag{15d}$$

where the nondimensional depth of the plenum chamber is given by $\bar{h} = h/\delta^*$. These boundary conditions provide four linear equations for the coefficients A_i, $i = 1, 2, 3, 4$. These were solved for the A_i using symbolic computing (MAPLE).

Using the linearized x-momentum equation, together with the boundary conditions (15a) and (15b) it can be shown that the pressure in the plenum chamber at $y = 0$ is given by

$$\hat{p}_s = i(\omega/\alpha)(A_1 - A_2) \tag{16}$$

If the expressions determined for A_1 and A_2 are substituted into Eq. (16) the following result is obtained for the admittance of the plenum chamber:

$$(Y_c)_{\sigma=1} = \hat{p}_c/\hat{q}_w = -i(\alpha/\omega)\Delta/N_1 \tag{17}$$

where

$$N_1 = \beta(\alpha+\beta)\left[e^{(\alpha-\beta)\bar{h}} - e^{-(\alpha-\beta)\bar{h}}\right] + \beta(\alpha-\beta)\left[e^{(\alpha+\beta)\bar{h}} - e^{-(\alpha+\beta)\bar{h}}\right] \tag{18}$$

$$\Delta = 8\alpha\beta + (\alpha-\beta)^2\left[e^{(\alpha+\beta)\bar{h}} + e^{-(\alpha+\beta)\bar{h}}\right] - (\alpha+\beta)^2\left[e^{(\alpha-\beta)\bar{h}} + e^{-(\alpha-\beta)\bar{h}}\right] \tag{19}$$

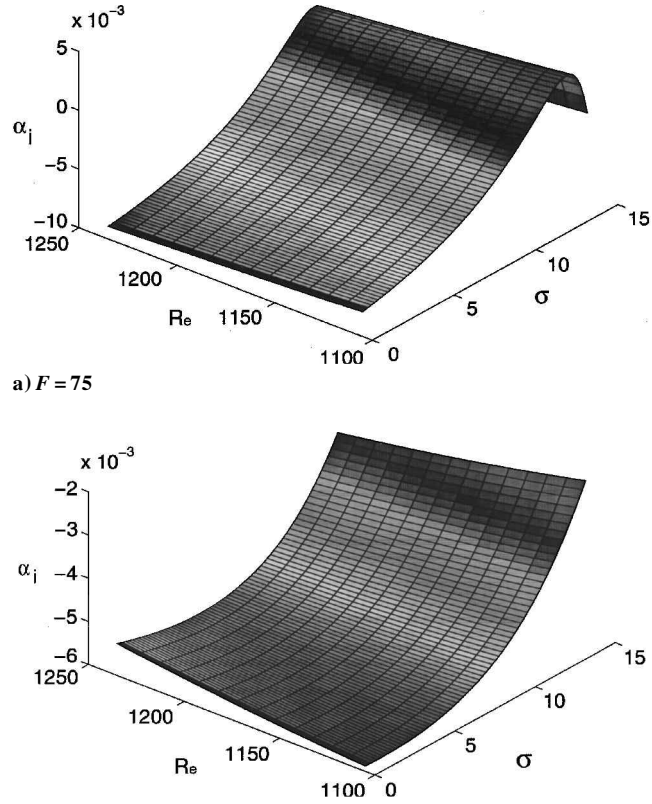

Fig. 4 Three-dimensional plots of α_i vs Reynolds number and porosity.

C. Numerical Study Using Theoretical Model of Admittance

The theoretical expression (17) for admittance can be used instead of a specified complex value with the numerical methods outlined in Sec. II to compute the corresponding eigenvalues and eigenfunctions when values of frequency and Reynolds number are given. In this way we carried out an extensive study of the effects of passive porous walls on boundary-layer stability, both at the higher dimensionless frequencies and lower Reynolds numbers appropriate to a parallel experimental study and for the values corresponding to Fig. 3, which are more appropriate for natural transition. In all cases it was found that the greatest stabilization was obtained for infinitely deep plenum chambers, although in practice there was little change for depths exceeding values of the order of the T–S wavelength. This seems to contradict the earlier results of Lekoudis,[9] although it is consistent with the flow physics described here earlier.

Some typical results corresponding to the experimental study are shown in Fig. 4. The variation of α_i with porosity σ over a small range of Reynolds numbers is plotted for two dimensionless frequencies. It can be seen that in both cases there is an optimum value of porosity for which the stabilization is greatest. For $F = 75$, it is around 0.12. The growth rate and dimensionless frequency corresponding to the most unstable T–S wave is plotted as a function of porosity in Fig. 5. It can be seen that at the selected Reynolds number of 1105 complete stabilization at all frequencies is achieved for a porosity slightly in excess of 0.16.

For the experimental study, a 90×90 mm porous panel is inset into a flat plate with its leading edge located 355 mm from the leading edge of the flat plate. The acoustic driver is located 205 mm from the plate's leading edge. At a flow speed of 20 m/s, this corresponds to $Re = 840$. Figure 6 presents a calculation of gain (the ratio of the local T–S amplitude to its value at $Re = 840$) for T–S waves driven at dimensionless frequencies of $F = 75$ and 85. The two vertical lines denote the leading and trailing edges of the porous panel. It can be seen that at $F = 75$ the 12% porosity panel completely stabilizes the T–S wave and partially stabilizes it at $F = 85$. Partial stabilization is seen for walls with lower values of porosity; Fig. 4a shows that the reduction in instability growth rate is

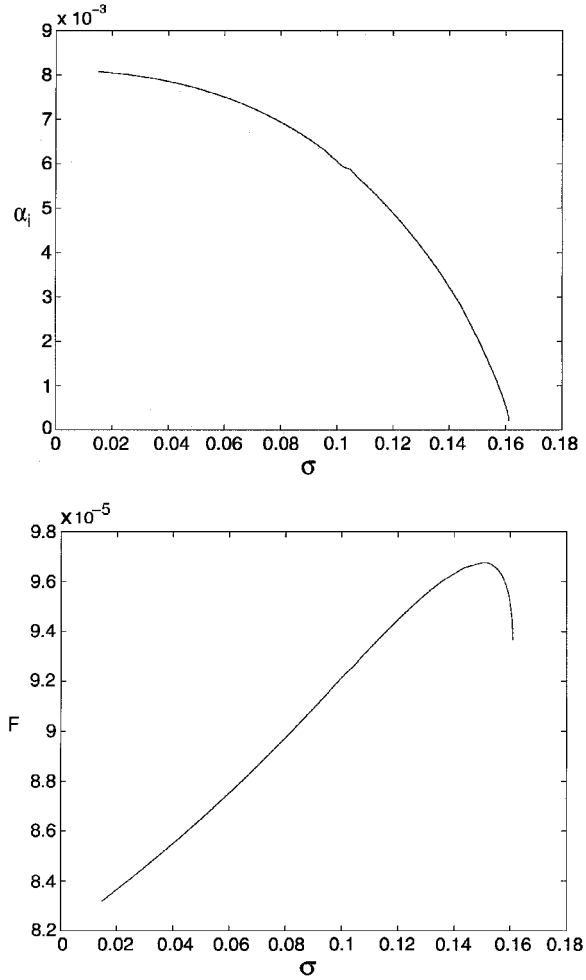

Fig. 5 Variation of growth rate and frequency with porosity for the most unstable mode; $Re = 1105$.

roughly proportionate to porosity up to the optimum value of about 12%. For porosities greater than this, the instability growth rate rises sharply.

To seek an explanation of the mechanisms responsible for the stabilization, we investigated the various terms in the integral disturbance energy equation. Following the procedure used by Carpenter,[2] Carpenter and Morris,[3] and others for disturbances propagating in boundary layers over compliant walls, we write the integral disturbance energy equation averaged over a cycle as

$$\frac{\mathrm{d}}{\mathrm{d}x}\left[\underbrace{\int_0^\infty \frac{U}{2}(\overline{u^2}+\overline{v^2})\,\mathrm{d}y}_{\text{(i)}} + \underbrace{\int_0^\infty \overline{up}\,\mathrm{d}y}_{\text{(ii)}} + \underbrace{\frac{1}{Re}\int_0^\infty \overline{v\omega}\,\mathrm{d}y}_{\text{(iii)}}\right]$$

$$= \underbrace{\int_0^\infty -\overline{uv}DU\,\mathrm{d}y}_{\text{(iv)}} + \underbrace{\overline{v_w p_w}}_{(v)} - \underbrace{\frac{1}{Re}\int_0^\infty \overline{\zeta^2}\,\mathrm{d}y}_{\text{(vi)}} \qquad (20)$$

where ζ is the perturbation vorticity. The term i on the left-hand side can be regarded as the total kinetic energy being convected past a given location. Terms ii and iii are the rates of flow work done by the perturbation stresses. Term iv is the rate of energy production by the Reynolds stresses. Term v is the rate of irreversible work done at the wall by the fluctuating pressure. Term vi is the rate of viscous dissipation. Differentiating term i with respect to x is equivalent to writing it as

$$-2\alpha_i \int_0^\infty \frac{U}{2}(\overline{u^2}+\overline{v^2})\,\mathrm{d}y$$

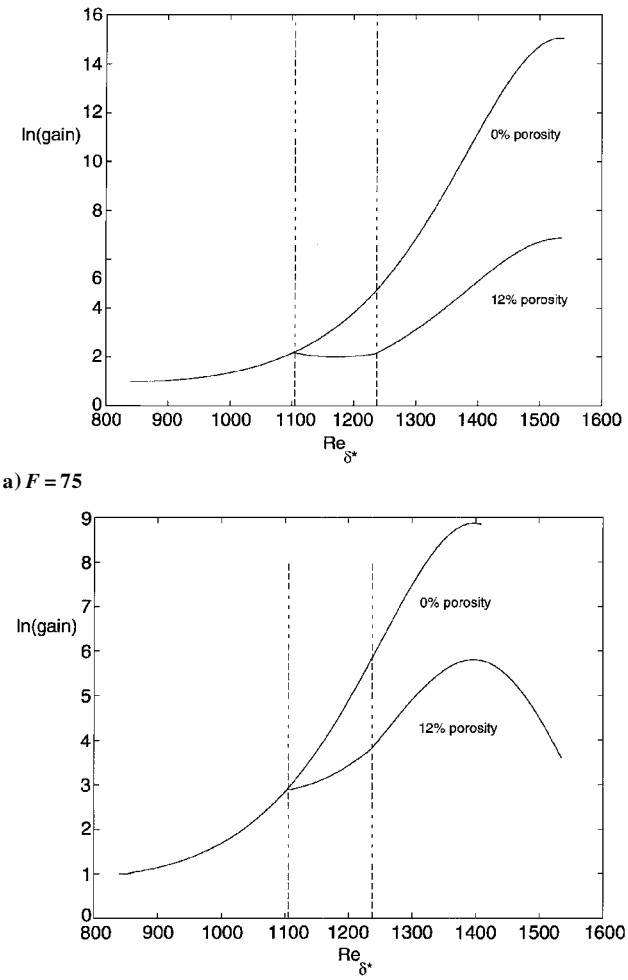

a) $F = 75$

b) $F = 85$

Fig. 6 Amplification plots for a rigid wall and a passive porous wall with $\sigma = 0.12$; wall is only porous between the vertical broken lines.

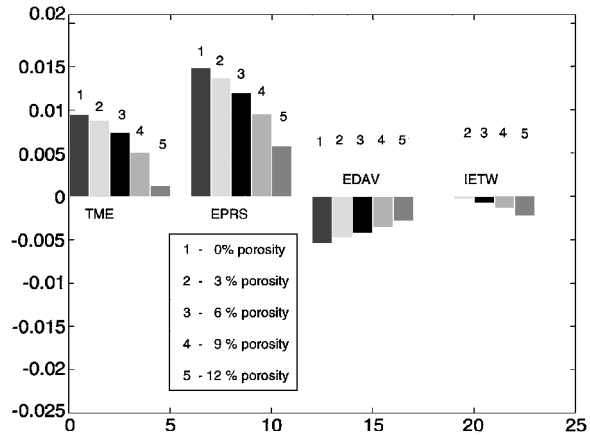

Fig. 7 Comparison of the magnitudes of the various terms in the energy equation (20) for a range of porosities; $F = 85$ and $Re = 1105$; TME, normalized total mechanical energy; EPRS, terms iv/i; EDAV, terms vi/i; and IETW, terms v/i.

The integrated mechanical energy, term i, is used to normalize the remaining terms to obtain the results plotted in Figs. 7 and 8.

Figure 7 shows the magnitudes of the normalized total mechanical energy, that is,

$$-2\alpha_i\left(1+\frac{\text{term ii} + \text{term iii}}{\text{term i}}\right)$$

and the normalized energy production rate, terms iv/i, the normalized rate of pressure work, terms v/i, and normalized dissipation

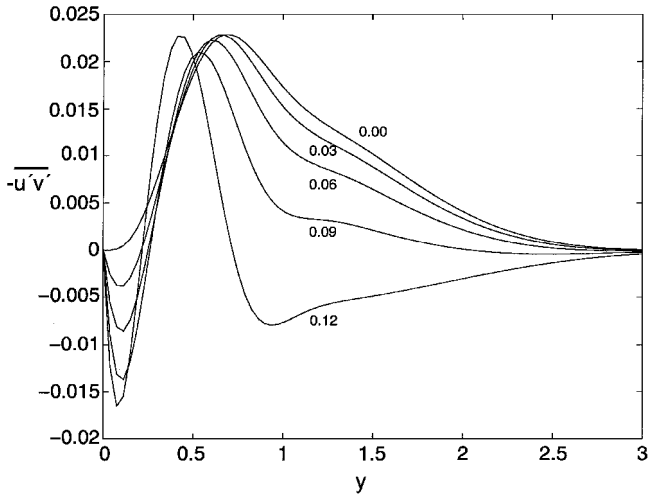

Fig. 8 Profiles of Reynolds stress across the boundary layer for various values of porosity: $F = 75$ and $Re = 1105$.

rate, terms vi/i, for the impermeable wall and porous walls with a range of porosities at $Re = 1105$ and dimensionless frequency, $F = 85$. As can be seen, the main stabilizing effect is the decrease in the energy production term as porosity rises; there is also a smaller favourable contribution due to the rise in the rate of irreversible pressure work at the wall. The distributions of Reynolds stress across the boundary layer are plotted in Fig. 8. It can be seen that a region of negative Reynolds stress develops adjacent to the wall and, to a lesser extent, in the outer part of the boundary layer as the wall porosity rises. This near-wall region of negative Reynolds stress appears to be the principal explanation for the stabilizing effect of passive porous walls predicted by the theory. The results shown in Figs. 7 and 8 correspond approximately to the conditions for the experimental investigation. Similar results were obtained at the Reynolds numbers and frequencies more appropriate to natural transition.

IV. Conclusions

A general inverse theory has been developed for passive porous walls that is based on classic linear stability theory. The porous wall is characterized by a complex admittance, the complex value reflecting the phase difference between the fluctuating driving pressure and the flow through the pores. It is found that passive porous walls characterized by an admittance phase very close to $\pi/2$ can completely stabilize T–S waves. This contrasts with compliant walls that stabilize T–S waves when the admittance phase is near to $-\pi/2$. It is also found that there exists an optimum magnitude of admittance that when exceeded leads to a rapid rise in the growth rate of the T–S waves.

A theoretical model for a practical passive porous wall has also been developed. This type of wall corresponds to a parallel experimental study and comprises a very thin porous sheet stretched over a plenum chamber. A theoretical expression for the admittance was derived for this type of porous wall. This was used with classic stability theory to predict the effect such a passive porous panel would have on the evolution of T–S waves in the experimental study. Strong stabilization was found for walls with 12% porosity. An investigation of the various terms in the integral disturbance energy equation revealed that the main stabilizing effect was due to greatly reduced energy production by the Reynolds shear stress. It emerged that as the porosity increases a region of negative Reynolds shear stress develops near the wall.

It remains to be seen whether the experimental study will confirm the theoretical predictions. There are several factors that could lead to problems in practice. For example, the theory requires the admittance phase to be very close to $\pi/2$. This can only be achieved in practice by minimizing the losses through the pores through using very thin tensioned metal sheet. Another area of concern is that the very weak pressure field generated by the T–S waves could be swamped by the quasi-random background noise. This could equally have been a problem with compliant walls. Yet Gaster[22] and Lucey and Carpenter[23] found very good agreement between the predictions of linear stability theory and experimental measurements of the evolution of disturbances in boundary layers over compliant panels. One may also anticipate difficulties if the pressure field is not sufficiently uniform along the passive porous panel. This might lead to areas of steady inflow and outflow, thereby modifying the undisturbed flowfield. Although nonuniform pressure fields could have led to steady deformations of compliant panels, thereby invalidating the measurements referred to earlier, they apparently did not. Last, it would be very difficult to measure the values of admittance in an experiment.

Acknowledgments

This work was carried with the support of British Aerospace plc. and a United Kingdom Engineering and Physical Science Research Council research grant. The authors would also like to acknowledge the helpful advice of M. Gaster.

References

[1]Schlichting, H., *Boundary Layer Theory*, 7th ed., McGraw–Hill, New York, 1979, pp. 499–554.

[2]Carpenter, P. W., "Status of Transition Delay Using Compliant Walls," *Viscous Drag Reduction in Boundary Layers*, edited by D. M. Bushnell and J. N. Hefner, Vol. 123, Progress in Astronautics and Aeronautics, AIAA, Washington, DC, 1990, pp. 79–113.

[3]Carpenter, P. W., and Morris, P. J., "The Effect of Anisotropic Wall Compliance on Boundary-Layer Stability and Transition," *Journal of Fluid Mechanics*, Vol. 218, 1990, pp. 171–223.

[4]Cooper, A. J., and Carpenter, P. W., "The Effect of Wall Compliance on Inflexion Point Instability in Boundary Layers," *Physics of Fluids*, Vol. 9, No. 2, 1997, pp. 468–470.

[5]Cooper, A. J., and Carpenter, P. W., "The Stability of Rotating-Disc Boundary-Layer Flow over a Compliant Wall. Part 1. Type I and II Instabilities," *Journal of Fluid Mechanics*, Vol. 350, Nov. 1997, pp. 231–259.

[6]Gaponov, S. A., "Influence of Porous Wall Properties on Boundary-Layer Stability," *Istvestiya Sibirskogo Otdeleniya Akademii Nauk SSSR*, No. 3, Pt. 1, 1971, pp. 21–23 (in Russian).

[7]Gaponov, S. A., "Stability of a Boundary Layer of Incompressible Fluid over a Slotted Surface," *Istvestiya Sibirskogo Otdeleniya Akademii Nauk SSSR*, No. 8, Pt. 2, 1975, pp. 37–42 (in Russian).

[8]Gaponov, S. A., "The Influence of Gas Compressibility on Boundary-Layer Stability over a Permeable Surface with a Subsonic Velocity," *Prikladnaya Matematika i Tekhnika Fizika*, No. 1, 1975, pp. 121–125 (in Russian).

[9]Lekoudis, S. G., "Stability of Boundary Layers over Permeable Surfaces," AIAA Paper 78-203, 1978.

[10]Carpenter, P. W., "The Feasibility of Using Passive Porous Walls for Drag Reduction," *Emerging Techniques in Drag Reduction*, edited by K.-S. Choi, T. V. Truong, and K. K. Prasad, Professional Engineering Publishing, Ltd., Bury St. Edmunds, England, U.K., 1996, pp. 221–242.

[11]Schetz, J. A., and Kong, F., "Turbulent Boundary Layer over Solid and Porous Surfaces with Small Roughness," AIAA Paper 81-0418, 1981.

[12]Wilkinson, S. P., "Influence of Wall Permeability on Turbulent Boundary-Layer Properties," AIAA Paper 83-0294, 1983.

[13]Collier, F. S., and Schetz, J. A., "Injection into a Turbulent Boundary Layer Through Porous Surfaces with Different Surface Geometries," AIAA Paper 83-0295, 1983.

[14]Nagamatsu, H. T., Orozco, R. D., and Ling, D. C., "Porosity Effect on Supercritical Airfoil Drag Reduction by Shock Wave/Boundary-Layer Control," AIAA Paper 84-1682, 1984.

[15]Breitling, R., and Zierep, J., "Computation of Transonic Viscous Flow over Airfoils with Control by Elastic Membrane and Comparison with Control by Passive Ventilation," *Acta Mechanica*, Vol. 87, Nos. 1–2, 1991, pp. 23–36.

[16]Beutner, T. J., Celik, Z. Z., and Roberts, L., "Computational Method for Describing Porous Wall Boundary Conditions Based on Experimental Data," *AIAA Journal*, Vol. 35, No. 9, 1997, pp. 1456–1463.

[17]Bechert, D. W., Bartenwefer, M., Hoppe, G., and Reif, W.-E., "Drag Reduction Mechanisms Derived from Shark Skin," *International Council for the Aeronautical Sciences*, ICAS Paper 86-1.8.3, 1986.

[18]Landahl, M. T., "On the Stability of a Laminar Incompressible Boundary Layer over a Flexible Surface," *Journal of Fluid Mechanics*, Vol. 13, 1962, pp. 609–632.

[19]Carpenter, P. W., and Garrad, A. D., "The Hydrodynamic Stability of Flow over Kramer-Type Compliant Surfaces. Part 1. Tollmien–Schlichting Instabilities," *Journal of Fluid Mechanics*, Vol. 155, 1985, pp. 465–510.

[20]Bridges, T. J., and Morris, P. J., "Differential Eigenvalue Problems in Which the Parameter Appears Nonlinearly," *Journal of Computational Physics*, Vol. 55, 1983, pp. 437–460.

[21]Sen, P. K., and Arora, D. S., "On the Stability of Laminar Boundary-Layer Flow over a Flat-Plate with a Compliant Surface," *Journal of Fluid Mechanics*, Vol. 197, 1988 , pp. 201–240.

[22]Gaster, M., "Is the Dolphin a Red Herring?," *Proceedings of the IUTAM Symposium on Turbulence Mangement and Relaminarisation,* edited by H. W. Liepmann and R. Narasimha, Springer, New York, 1987, pp. 285–304.

[23]Lucey, A. D., and Carpenter, P. W., "Boundary Layer Instability over Compliant Walls: Comparison Between Theory and Experiment," *Physics of Fluids*, Vol. 7, No. 10, 1995, pp. 2355–2363.

P. J. Morris
Associate Editor